NANO EXPRESS   **Open Access**

CrossMark

The Computational Studies of Plasmon Interaction

Antonina Demchuk[*] , Ivan Bolesta, Oleksii Kushnir and Ihor Kolych

Abstract

In this paper, an interaction of metal nanoparticles that appears in the extinction spectra was investigated. The mutual coupling between the nanoparticles, the effect of size difference, and the interparticle separation in silver nanoparticle dimers are studied by computer discrete dipole approximation methods. The obtained results show that nanoparticle interaction results in the distinct collective modes, known as the low-energy bonding modes and the higher-energy antibounding modes. The spectral position of the modes is analyzed as a function of the ratio of interparticle distance to particle size that reduces the dependency on the particle size itself. The optical spectra of nanoparticles that form the fractal cluster were investigated. It was found that the number of spectral bands increase with the growth of the number of nanoparticles in the fractal cluster, which are described within the plasmon hybridization model.

Keywords: Nanoparticle, Surface plasmon resonance, Optical spectra, Extinction cross section, Hybridization model, Dimer, Fractal cluster, Discrete dipole approximation

Background

Metal nanoparticles have attracted a great attention due to their strong interaction with light. The interesting optical properties of metal nanoparticles, such as bright intense colors, are the result of interaction of free carriers with the incident electric field. In the presence of the oscillating electromagnetic field of the light, the free electrons of the metal nanoparticle undergo a collective coherent oscillation with respect to the positive metallic lattice [1]. This process is resonant at a particular frequency of the light and is called the localized surface plasmon resonance (LSPR) oscillation.

In a single metal nanoparticle, frequency, strength, and quality of the LSPR depends on the size, geometry, the metal composition, and the refractive index of the local environment. Furthermore, the LSPR of a metal nanoparticle is sensitive to the presence of other nearby metal nanoparticles, their sizes, interparticle distance, and materials. In an assembly of metal nanoparticles with small interparticle distance compared to the size of particle, the LSPR is strongly affected by the near-field coupling of the individual particles [2].

Another aspect of the study is the plasmon spectra of metal nanoparticles associated with the formation of metal-dielectric nanocomposites. Nanocomposites can cause significant influence on linear and nonlinear susceptibilities of matrix [3], radiation recombination processes [4], and giant surface-enhanced Raman scattering (SERS)[5]. Practical interest in dielectric materials with metal nanoparticles is connected with perspective for development of optical switches on their basis with ultrashort time response, limiters of optical laser beam intensity, for synchronization of the laser modes, etc.

Progress in the investigation of plasmonic spectra of the metal nanoparticles has been greatly assisted by developments in technology, experimental techniques, and numerical modeling of their extinction spectra. This allows to study the impact of different factors on the extinction spectra of nanoparticles and their composites.

Pairs of nanoparticles called "dimers" are the simplest model systems to study as only two directions of incident polarization required to explore the interparticle coupling completely. It is shown [6] that dimers with an interparticle distance smaller than the diameter of the nanoparticles can generate high plasmonic enhancements.

The optical spectra of individual particle, dimers and the chains consisting of particles of the same size, the dependence on the medium host, the interparticle separation,

*Correspondence: demchuk.antonina@gmail.com
Department of Radiophysics and Computer Technologies, Ivan Franko
National University of Lviv, Generala Tarnavskoho Str. 107, 79017, Lviv, Ukraine

Demchuk *et al. Nanoscale Research Letters* (2017) 12:273

Page 2 of 7

and the direction of incident polarization were studied in [7]. The authors of [8] explored the extinction spectra and plasmon hybridization schemes of nanoparticle dimers of various sizes and materials. In [9], the field enhancement spectra were investigated as a function of the particle size difference and the interparticle spacing, and also, localized surface plasmon resonances in the chains of different particle sizes were analyzed depending on the particle size and interparticle separation [10].

The general case of the spherical nanoparticle coupling is fractal clusters. Since fractal clusters are characterized by local anisotropy of each particle surroundings, the supplements compensation to local field (including the dominant surroundings contribution) do not occur. This leads to the emergence of strong local electromagnetic fields, which will vary in different parts of fractal cluster (field fluctuation)[11]. Local fields, in turn, enhance the optical susceptibilities of particles that reflects in the linear and nonlinear optical characteristics of fractal clusters [12]. As a result, the extinction spectra of fractal clusters differ significantly from the spectra of individual material nanoparticles.

This paper studies the nanoparticle interaction that shows up in the extinction spectra. The spectra of the simple nanoparticle system (dimers with particles of similar and dissimilar sizes) were analyzed. The changes of spectra are investigated to depend on the interparticle distance and the interaction of particles as the part of fractal cluster.

Methods

We use the discrete dipole approximation (DDA) method to simulate the distribution of the electromagnetic field for the composition of silver nanoparticles. Extinction cross sections are calculated from the resulting polarizations of DDA method, using the solving package "EMSimulation" [13]. The dielectric function of silver nanoparticles is taken as a bulk silver from the Johnson and Christy table [14] with phenomenological correction for size reduction effects. The particles are assumed to be embedded in a vacuum, which is described by a relative permittivity $\varepsilon = 1$ or in dielectric media with $\varepsilon = n^2$, where n is the refractive index.

The DDA is a method for calculating scattering and absorption of electromagnetic waves by nanocomposites. The DDA was proposed in 1973 by Purcell and Pennypacker [15], who used it to study interstellar dust grains. The main idea of the method is that the target is approximated by an array of N point dipoles at positions r_i with polarizabilities a_i. The polarization

$$P_i = a_i \cdot E(r_i) \tag{1}$$

of each dipole responds to the total electric field at its position; $E(r_i)$ is the sum of an incident plane wave

$$E_{\text{inc},i} = E_0 \exp(ik \cdot r_i - i\omega t) \tag{2}$$

and a contribution from all the other dipoles

$$E_{\text{other},i} = -\sum_{i \neq j} A_{ij} \cdot P_j. \tag{3}$$

The medium of the target is characterized by its complex dielectric function ε. The dipole polarizabilities a_i can be given by the Clausius-Mosotti polarizability [16]:

$$a_i = \frac{3d^3}{4\pi} \left(\frac{\varepsilon_i^2 + 1}{\varepsilon_i^2 + 2} \right), \tag{4}$$

where d is the diameter of the dipole. Draine [17] showed that for finite wavelengths, the optical theorem requires that polarizabilities include also the radiative-reaction correction of the form

$$\alpha = \frac{\alpha^{(nr)}}{1 - (2/3)i(\alpha^{(nr)}/d^3)(kd)^3}, \tag{5}$$

where $\alpha^{(nr)}$ is the nonradiative polarizability.

The DDA method allows to get an oscillating dipole moments P_j for every monochromatic incident wave; from these P_j the absorption and scattering cross sections are computed [18]:

$$C_{ext} = \frac{4\pi k}{|E_0|^2} \sum_{j=1}^{N} Im \left(E_{inc,j}^* \cdot P_j \right) \tag{6}$$

$$C_{abs} = \frac{4\pi k}{|E_0|^2} \sum_{j=1}^{N} \left\{ Im \left(P_j \cdot \left(\alpha_j^{-1} \right)^* P_j^* \right) - \frac{2}{3} k^3 |P_j|^2 \right\} \tag{7}$$

To compare cross sections of dipoles with different radiuses, we use effective cross sections, which are calculated as

$$Q_{\text{ext}} = C_{\text{ext}}/A, \tag{8}$$

$$Q_{\text{abs}} = C_{\text{abs}}/A, \tag{9}$$

where A is the area of overlap between the incident beam and the target object.

The scattering problem for the array of point dipoles, represented by the system of linear equation, can be solved with arbitrary accuracy. We use the fast Fourier transform (FFT) techniques together with the conjugate gradient method to obtain solutions for targets.

We calculated extinction spectra of fractal clusters with increasing degree of aggregation of nanoparticles in the clusters. Simulations of fractal clusters growth conducted in a "cluster-cluster" model [19].

To decompose the optical spectra into peak functions, we performed two steps. Firstly, the method of second derivative spectroscopy [20] was used to find the hidden peaks for the initial definition of the peak position. Then,

L-BFGS (Broyden-Fletcher-Goldfarb-Shanno) [21] algorithm was used to reduce the standard deviation between the peak superposition and the simulated spectrum of fractal cluster.

Results and Discussion

Calculation of extinction spectra of dipoles shows that the interaction between the nanoparticles, which depends on the distance between them, manifested in the appearance of two components (Fig. 1). Spectral distance $\Delta\lambda$ between components depends on the distance (D) between nanoparticles (for fixed radius r), on the size of nanoparticles (for fixed distances), and on the permittivity of the environment.

In the case of dielectric medium other than vacuum, the behavior of the spectra remains qualitatively the same, but the band shifted to long wavelength region (for isolated particles and dimers) and splitting between the bands increases. Analysis of the results shows that the ratio $d = D/r$ is more universal because it minimizes the dependency on the nanoparticle radius r.

Figure 1 shows effective cross section extinction spectra of dimer in vacuum with similar size particles with radius $r = 10$ nm dependent on interparticle separation d, where $d = D/r$ depends on the radius of a nanoparticle r and the interparticle distance D (Fig. 1a). Cross section extinction was calculated under the longitudinal, transverse, and oblique incident field polarization. Both the longitudinal and transverse plasmon coupling bands for the homodimer can be recognized under the oblique polarization.

Calculation results show that at the interparticle separation $d > 2$, only one strong plasmon coupling absorption band can be observed. After decreasing the interparticle distance, the single plasmon resonance band is split into two plasmon bands forming two different peaks (Fig. 1b).

When the gap distance between nanoparticles is large enough, every metal nanoparticle exists as an individual, so the interaction between nanoparticles is very weak. When the gap is quite small, the system of nanoparticles consider to be as a whole. So in both cases, it is impossible to cause the energy splitting and the resonance peak position shifting.

Moreover, the plasmon coupling of a dimer shows a large red-shift as the interparticle distance decreases for incident polarization parallel to the dimer axis, due to the applied and induced electric fields that are added to each other. For incident polarization perpendicular to the axis, a destructive interaction between the applied and induced electric fields is predicted, leading to a small blue spectral shift [22].

The extinction spectrum of a symmetric dimer displays two distinct modes (Fig. 2a), the lower energy one at 374.2 nm resulting from the longitudinal coupling of the particle plasmons and the higher-energy one at 349.7 nm from the transverse coupling.

This behavior in electromagnetic coupling of the plasmon resonance between two nanoparticles can be explained by the phenomenon of molecular hybridization. This means when very strong plasmonic enhancement is in place within a dimer, two plasmons hybridize to form a lower energy bonding plasmon mode and a higher-energy antibonding plasmon mode [23].

In order to demonstrate the effect of introducing a size asymmetry in the coupling scheme, we discuss the LSPR scattering spectra obtained from an asymmetric dimer composed of a 4- and 10-nm silver particle.

The extinction spectra were calculated (Fig. 2b) for two extreme orthogonal polarizations of the asymmetric dimer, each contains two modes at 350.8 and 358.9 nm for the transverse and at 347.5 and 367.6 nm for the longitudinal polarization, respectively. This observation is in
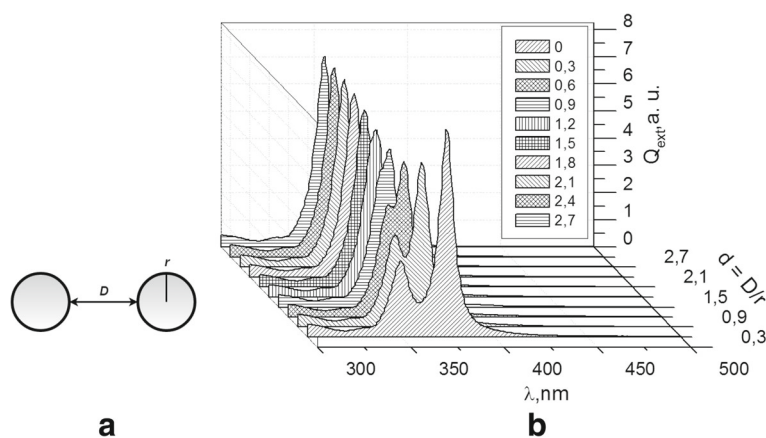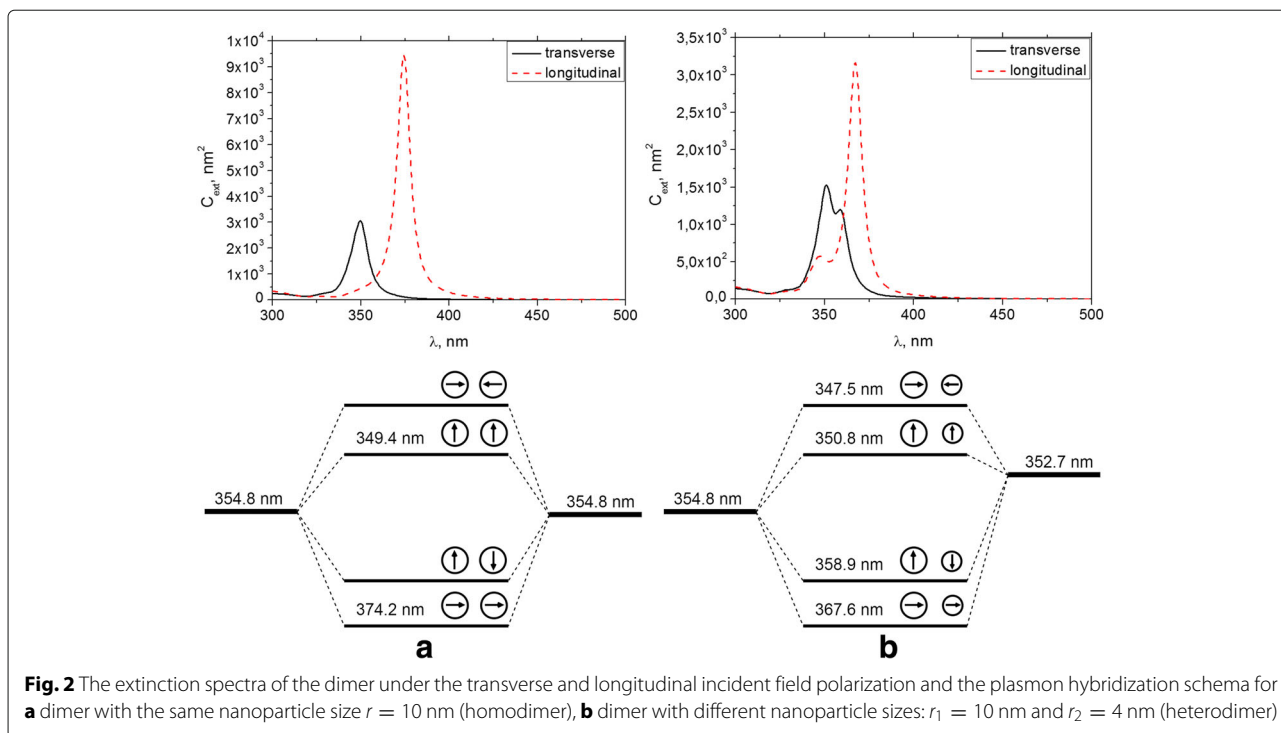

Fig. 1 a The dimer with nanoparticle radius *r* and interparticle distance *D*. **b** The effective extinction spectra of nanoparticle dimer dependent on the interparticle separation *d*

Demchuk *et al. Nanoscale Research Letters* (2017) 12:273

Page 4 of 7

Fig. 2 The extinction spectra of the dimer under the transverse and longitudinal incident field polarization and the plasmon hybridization schema for **a** dimer with the same nanoparticle size $r = 10$ nm (homodimer), **b** dimer with different nanoparticle sizes: $r_1 = 10$ nm and $r_2 = 4$ nm (heterodimer)

direct contrast to the homodimer case (Fig. 2a) and can be understood by introducing the asymmetry in the plasmon hybridization model, as depicted in the hybridization scheme.
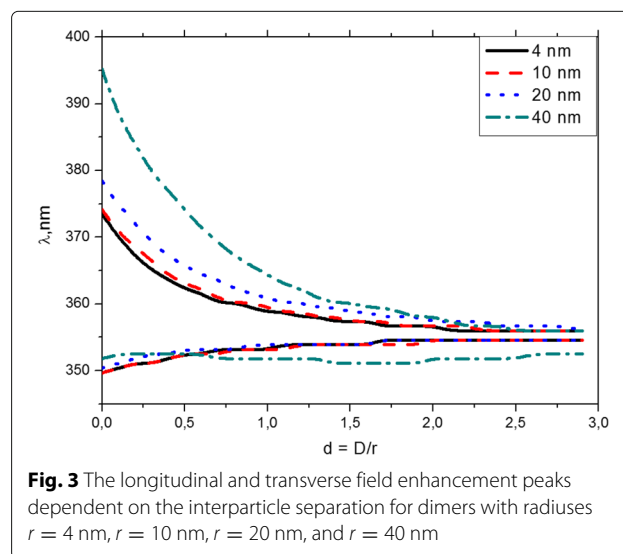
When the sizes of nanoparticles in the system are different, the electric field can no longer be assumed to be uniform inside the particles, and high-order (quadrupole, octupole, etc.) plasmon modes can directly couple with the electric field of the light simply due to the phase retardation effect. Excitation of multipole plasmon resonances is the result of the asymmetric distribution of the surface plasmons caused by the electromagnetic interactions between the localized modes. This effect may be used to enhance the nonlinear optical response of an effective medium composed of particles with engineered size dispersion and particle placement [10].
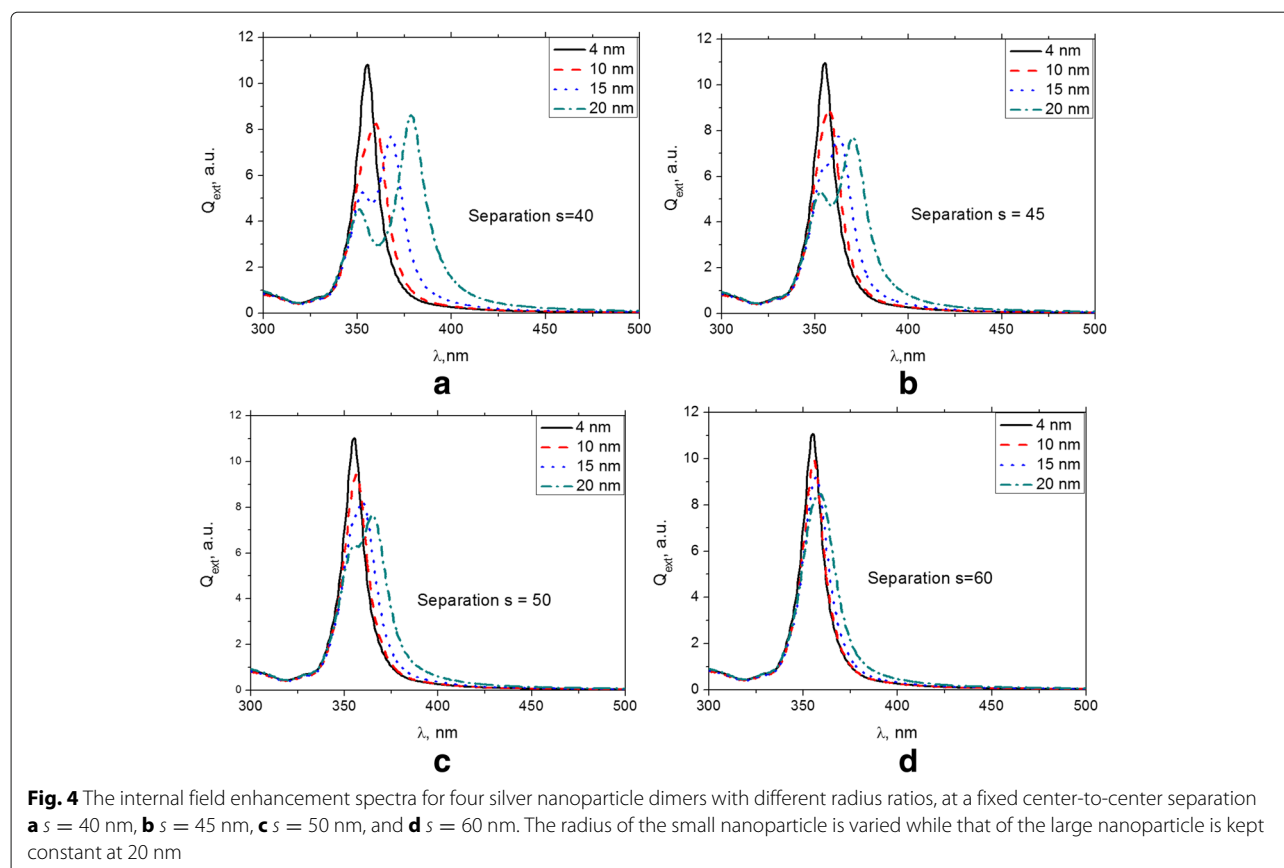
Figure 3 shows relation of the longitudinal and the transverse field enhancement peak to interparticle separation for different radiuses of nanoparticles in the homodimer. The figure shows the exponential relationship between the position of the peak enhancement and the interparticle distance of dimer with the asymptotical approaching the wavelength value 354.8 nm that corresponds to the isolated sphere enhancement.

The spectral distance $\Delta\lambda$ between the enhancement peaks follows a universal scaling law as a function of the dimensionless parameter $d = D/r$ (quasi-exponential behavior) and has given birth to the concept of "plasmon ruler" that may be used to infer the

length of a molecular chain connecting functionalized nanoparticles.

Figure 4a show the results for a dimer with a different radius ratio. The radius of the small nanoparticle is varied while that of the large nanoparticle is kept constant at 20 nm. The field enhancement shows two resonance peaks for the lower radius ratio. At a larger volume ratio, the peak field enhancement has increased. With increase in interparticle spacing, the peak enhancement shifts to

Fig. 3 The longitudinal and transverse field enhancement peaks dependent on the interparticle separation for dimers with radiuses $r = 4$ nm, $r = 10$ nm, $r = 20$ nm, and $r = 40$ nm

Demchuk *et al. Nanoscale Research Letters* (2017) 12:273

Page 5 of 7

Fig. 4 The internal field enhancement spectra for four silver nanoparticle dimers with different radius ratios, at a fixed center-to-center separation **a** $s = 40$ nm, **b** $s = 45$ nm, **c** $s = 50$ nm, and **d** $s = 60$ nm. The radius of the small nanoparticle is varied while that of the large nanoparticle is kept constant at 20 nm

lower wavelengths and shows less pronounced peak splitting. The smaller separation leads to an increased field enhancement due to the larger near field provided by the bigger size particle at this distance.

For small size difference or large interparticle spacing, low-field enhancement peaks are observed. For most geometries, the field enhancement peak exceeds that of an isolated silver nanoparticle, with the exception of dimers with small radius ratio or large interparticle spacing. The largest field enhancement peaks are observed at small spacing and large size difference.

We calculated the extinction spectra of nanoparticles which form the fractal cluster. Simulation of fractal cluster growth was carried out from 1000 polydisperse nanoparticles within the model of "cluster-cluster" (Fig. 5a), which corresponds to the natural growth of fractal aggregates in sols. The radius of nanoparticles is normally distributed with the mean of 5 nm and the dispersion of 1 nm.

Figure 5b presents the change (dynamics) of the extinction cross section spectra within the fractal grows stages. Curve 1 shows the spectrum of non-interacting particles, curves 2—11 show the spectra of clusters, with increasing number of particles respectively, curve 12 shows the spectrum of fractal clusters with all joined nanoparticles.

Analysis of the spectra by derivative spectroscopy method revealed the number of spectral components (peak functions) in the cluster (Fig. 6a). It is shown that the number of spectral components increase with the growth of the number of nanoparticles in the fractal cluster at different stages of cluster formation.

On the spectrum of non-interacting nanoparticles (aggregation step 1), one band with a maximum at 3.18 eV can be observed (curve 5 at Fig. 6a). The spectra of the initial stages of cluster formation (aggregation steps 2 and 3) show the additional three bands with the maximum at 2.60, 2.83, and 3.36 eV (curves 2, 4, and 6 in Fig. 6a). At the later stages of aggregation, the additional bands at 2.45 and 3.52 eV are present (curves 1 and 7 in Fig. 6a).

Figure 6a shows that the spectral position of the component in spectra does not depend on the degree of aggregation. For most components, the band energy does not change significantly at different stages of cluster formation. For the low-energy components (curves 1 and 2 in Fig. 6a), we can observe large red-shift with the growth of cluster, and for the high-energy components (curve 6, 7 in Fig. 6a), small blue-shift is present. This phenomenon can be explained by interaction of large number of nanoparticles in cluster and corresponds to the previously obtained results for the simple system of nanoparticle dimer.
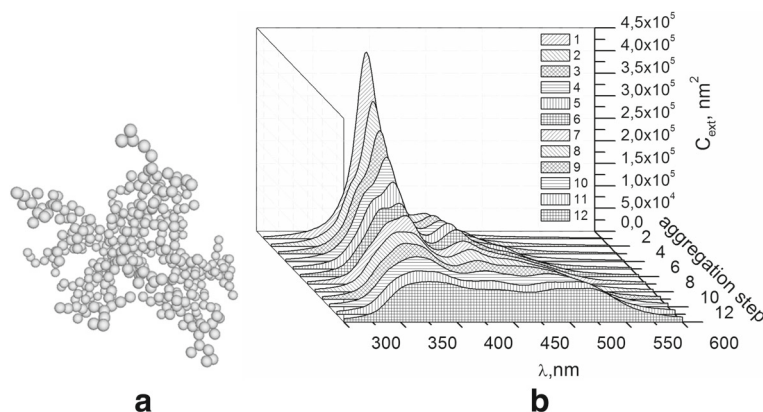
Demchuk *et al. Nanoscale Research Letters* (2017) 12:273

Page 6 of 7

Fig. 5 a The fractal cluster simulated within the model of "cluster-cluster." **b** Extinction spectra of the nanoparticles at different stages (curves 1–12) of fractal cluster formation

The difference between the extinction spectra of fractal clusters and non-interacting spectra is shown on the hybridization scheme on Fig. 6b. Low-energy bands at 2.60 and 2.83 eV can be associated with bounding orbitals corresponding to different orientations of interacting dipoles. High-energy bands at 3.36 and 3.52 eV are associated with loosening plasmon modes. Moreover, the most high-energy mode appears in clusters with sufficiently large number of particles (curve 7 at Fig. 6a).

Dipole-dipole interaction of nanoparticles can cause splitting in the energy modes, as shown in hybridization schema (Fig. 6b). The low energy band at 2.45 eV does not correspond to dipole mode interaction and can appear at higher levels of aggregation, as a result of high-order modes interaction (quadrupole, octupole, etc.).

Conclusions

In summary, the optical properties of plasmon resonant metal nanocomposites were investigated. Plasmon resonances are numerically evaluated in the silver nanosphere dimers of similar and different sizes and in the fractal cluster containing silver nanoparticles embedded in a vacuum.

We have shown that the interparticle coupling interaction among the random distribution of silver nanoparticles can lead to hybridization, splitting, and shifting of the plasmon energies, as well as the quadrupolar resonances formed by the interaction between the plasmons of the metal nanoparticles.

The extinction spectra in dimers with identical nanoparticle sizes indicate the presence of a dipolar particle response. However, the interaction of particles with dissimilar sizes also results in the splitting of the plasmon resonances into two resonances: the lower energy bounding plasmon and the higher-energy antibounding plasmon.

The change of the maximum band as a function of the particle size and interparticle separation was analyzed. It is shown that the maximum band depends on the ratio of the interparticle distance to the size of particles, and
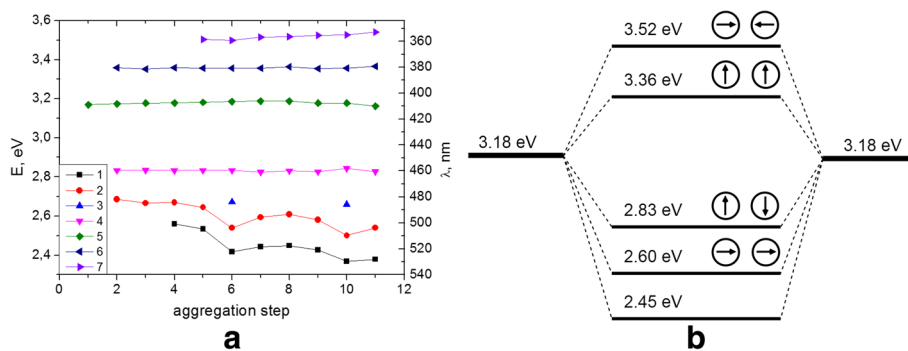

Fig. 6 a The spectral position of components at different stages of cluster formation. The numbers on the horizontal axis correspond to the numbers of curves in Fig. 5. **b** The hybridization scheme of plasmon modes in fractal cluster

Demchuk *et al. Nanoscale Research Letters*   (2017) 12:273

Page 7 of 7

this relation is more universal because it minimizes the dependency on the nanoparticle size.

In the fractal cluster consisting of similar nanoparticles the additional energy modes can appear that indicates the presence of higher-order plasmon modes (quadrupole or higher). The spectral position of maximum bands does not change significantly with the degree of aggregation of cluster. But the higher modes mostly appears on the later stages of fractal cluster formation.

The obtained results can be used for analyzing the real nanocomposites, determining the interparticle distance between nanoparticles, and creating the nanomaterials with special properties.

Abbreviations
DDA: Discrete dipole approximation; FFT: Fast-fourier transform; L-BFGS: Limited-memory Broyden-Fletcher-Goldfarb-Shanno; LSPR: Localized surface plasmon resonance; SERS: Surface-enhanced Raman scattering

Authors' Contributions
AD implemented the computer simulation methods, calculated the optical spectra of dimers, performed the data processing, and worked on the manuscript. IB was responsible for the conception of the work, data analysis, interpretation of the results, and final approval of the manuscript. OK provided the data processing and analysis, created the graphical plots of the calculated spectra, and worked on the manuscript. IK contributed to the implementation of the DDA method, simulated the fractal cluster structures, and calculated the optical spectra of the clusters. All authors read and approved the final manuscript.

Competing Interests
The authors declare that they have no competing interests.

Publisher's Note
Springer Nature remains neutral with regard to jurisdictional claims in published maps and institutional affiliations.

References
1. Kreibig U, Vollmer M (1995) Optical properties of metal clusters. Springer Science & Business Media, Berlin
2. Bohren CF, Huffman DP (1983) Absorption and scattering of light by small particles. Wiley, New York
3. Shalaev VM (1996) Electromagnetic properties of small-particle composites. Phys Rep 272:61–137
4. Blanco LA, de Abajo FJG (2004) Spontaneous emission enhancement near nanoparticles. J Quant Spectrosc Radiative Transf 89:37–42
5. Stockman MI, Shalaev VM, Moskovits M, Botet R, George TF (1992) Enhanced Raman scattering by fractal clusters: scale-invariant theory. Phys Rew B 46(5):2821–2830
6. Ji X, Yang W (2014) High-purity gold nanocrystal dimers: scalable synthesis and size-dependent plasmonic and Raman enhancement. Chem Sci 5:311–323
7. Mamoun W (2011) Discrete-dipole-approximation (DDA) study of the plasmon resonance in single and coupled spherical silver nanoparticles in various configurations [Master's thesis]. Concordia University
8. Sheikholeslami S, Jun YW, Jain PK, Alivisatos AP (2010) Coupling of optical resonances in a compositionally asymmetric plasmonic nanoparticle dimer. Nano Lett 10(7):2655–2660
9. Toroghi S, Kik PG (2012) Cascaded plasmon resonant field enhancement in nanoparticle dimers in the point dipole limit. Appl Phys Lett 100(18):183105
10. Toroghi S, Kika PG (2011) Design of cascaded plasmon resonances for ultrafast nonlinear optical switching. SPIE Proc 8054:80540E
11. Rechberger W, Hohenau A, Leitner A, Krenn JR, Lamprecht B, Aussenegg FR (2003) Optical properties of two interacting gold nanoparticles. Optics Commun 220:137–141
12. Kneipp K, Wang Y, Kneipp H, Perelman L, Itzkan I, Dasari R, et al (1997) Single molecule detection using surface-enhanced Raman scattering (SERS). Phys Rev Lett 78:1667–1670
13. ToniaDemchuk (2016) EMSimulation . https://github.com/ToniaDemchuk/EMSimulation. Accessed 15 Dec 2016
14. Johnson PB, Christy RW (1972) Optical constants of the noble metals. Phys Rev B 6:4370–4379
15. Purcell EM, Pennypacker CR (1973) Scattering and absorption of light by nonspherical dielectric grains. Astrophys J 186:705–714
16. van de Hulst HC (1981) Light scattering by small particles. Dover Publications, New York
17. Draine BT (1988) The discrete-dipole approximation and its application to interstellar graphite grains. Astrophys J 333:848–872
18. Draine BT, Flatau PJ (1994) Discrete-dipole approximation for scattering calculations. J Opt Soc Am A 11:1491–1499
19. Jullien R, Botet R (1987) Aggregation and fractal aggregates. World Scientific Pub Co Inc, Singapore
20. Dubrovkin IM, Belikov VG (1988) Derivative spectrophotometry, theory, technique, application. Rostov University
21. Zhu C, Byrd RH, Lu P, Nocedal J (1997) Algorithm 778: L-BFGS-B: Fortran subroutines for large-scale bound-constrained optimization. ACM Trans Math Softw 23:550–560
22. Jain PK, Lee KS, El-Sayed IH, El-Sayed MA (2004) Calculated absorption and scattering properties of gold nanoparticles of different size, shape, and composition: applications in biological imaging and biomedicine. J Phys Chem B 110(14):7238–7248
23. Nordlander P, Oubre C, Prodan E, Li K, Stockman MI (2004) Plasmon-induced transparency in metamaterials. Nano Lett 4(5):899–903